

# Experimental and Numerical Studies of Drag Reduction on a Circular Cylinder

A.O. Ladjedel, B.T.Yahiaoui, C.L.Adjlout and D.O.Imine

**Abstract**—In the present paper; an experimental and numerical investigations of drag reduction on a grooved circular cylinder have been performed. The experiments were carried out in closed circuit subsonic wind tunnel (TE44); the pressure distribution on the cylinder was conducted using a TE44DPS differential pressure scanner and the drag forces were measured using the TE81 balance. The display unit is linked to a computer, loaded with DATASLIM software for data analysis and logging of result. The numerical study was performed using the code ANSYS FLUENT solving the Reynolds Averaged Navier-Stokes (RANS) equations. The  $k-\epsilon$  and  $k-\omega$  SST models were tested. The results obtained from the experimental and numerical investigations have showed a reduction in the drag when using longitudinal grooves namely 2 and 6 on the cylinder.

**Keywords**—Circular cylinder, Drag, grooves, pressure distribution

## I. INTRODUCTION

FLOW around a circular cylinder was intensively studied in the past and that returns to its simple geometry as well as the logical structure of the vortices. The studies were led on the one hand by academic interest and on the other hand by practical interest (industrial).

In general the techniques of control of flow around a cylinder for the reduction of the drag are classified in two types; indicated under the name of “active and passive control”. The active control methods order the flow by ensuring external energy by means such as the acoustic excitation or the jet blow. The passive control methods order the flow by modifying the shape of the body or by attaching additives devices such as elements of roughness on the body SAKAMOTO et al [1], N. Fujisawa, G. Takeda [2]. The active control requires complex mechanics devices which provide the external power to the flow consequently, the passive method is simpler and easier to realize.

A.O.LADJEDEL, laboratoire d'aérohydrodynamique naval Département de génie maritime, mechanical engineering faculty, USTO Oran 31000 Algeria (e-mail: ladjedelomar@yahoo.com)

B.T.Yahiaoui Laboratoire d'aéronautique et systèmes propulsive, Département de Génie Mécanique, Mechanical Engineering Faculty, USTO Oran, 31000 Algeria, (e-mail:yahiaoui\_tayeb@yahoo.fr)

C.L.ADJLOUT, laboratoire d'aérohydrodynamique naval Département de génie maritime, mechanical engineering faculty, USTO Oran 31000 Algeria (e-mail: adjloutl@yahoo.fr)

D.O.IMINE Laboratoire d'aéronautique et systèmes propulsive, Département de Génie Mécanique, Mechanical Engineering Faculty, USTO Oran, 31000 Algeria, (e-mail: imine\_omar@yahoo.fr)

Many studies about passive control techniques exist as the approach of Igarashi and Tsutsui [3, 4], who have installed a trip-wire in the separate shearing layer of a cylinder for a Reynolds number  $Re = 4.2 \times 10^4$ . The addition of this wire reduced the mean drag force acting on the cylinder by 20–30%, where the greatest reduction of drag is being obtained when a trip-wire was located under an angle of  $120^\circ$  at the stagnation point. Park and lee [5], Lee and Lee [6], Igarashi and Tsutsui [7,8] have also studied the effect of installing a small-diameter control rod within the separated shear layer formed around the main cylinder and the effect of the Reynolds number variation on the reduction of the drag. Mahir and Rockwell [9] studied the wakes behind an arrangement side by side (side-by-side) of two cylinders subjected to various excitations.

It is well-known that the drag in a cylinder decreases when the wake behind it changes laminar flow with turbulent with a narrow wake width. Zdravkovich [10] suggested a method for reducing drag by using an obstacle placed upstream or downstream to alter the flow field around the bluff body. Igarashi [11] reported that the drag on a square prismatic cylinder was reduced from 50 to 70% by the installation of a small-diameter control rod upstream of the cylinder for the Reynolds number  $Re = 3,2 \times 10^4$ . He investigated the interaction between the shear flow separated from the control rod and the square prism. Mittal et al [12] carried out a numerical investigation for the reduction of the drag on the rear cylinder of two identical cylinders arranged in tandem. They noted that the drag on this cylinder was reduced approximately 40% when the two cylinders were gaped with a distance from 1.5D. Sakamoto and Haniu [13] studied the suppression of the fluid forces acting on a cylinder when a control rod was added to the system. They remarked that the time-averaged mean drag force could be reduced until approximately to 50%, and that the drag forces could be reduced up to 85% by using a control rod.

This type of study of the grooved walls has touched different domains such as the aeronautical industry where, the grooved walls are installed on the aircraft; the purpose of these grooves is to reduce drag. E.Coustols [14] has studied the effect of the grooved walls on the structure of a turbulent boundary layer, he has tested a various forms of grooves as triangular in “V”, in the form of “U” and also in the form of “L”, in these three kinds of grooves, he noted that the “L” form had reduced the drag about 10%. The idea to make grooves on the cylinder is also from a study made by S.Alley and G.Ungal [15] they noticed that the plants of cactus have a strong resistance against the wind forces and that returns to their longitudinal grooves.

The flow around a bluff body is distinctively different, depending on the geometrical shape and surface condition of the body. The possible drag reduction and the corresponding variation of the flow field around a circular cylinder are studied in a wind tunnel using flow control by adding grooves to the examined cylinders and simulated numerically by using the code ANSYS Fluent.

II. EXPERIMENTAL FACILITY

A. Setup

The Wind Tunnel shown in figure 1 is of the closed circuit, horizontal return type with a working section 460 mm high, 460 mm, wide and 1200 mm long. The Closed Circuit Wind Tunnel is of conventional design and has advantages over a similar open circuit design. These include; a higher maximum velocity, lower power consumption and lower noise level. It is driven by an A.C motor and axial flow fan that forces air around the circuit and produces a maximum velocity of 60 m/s.

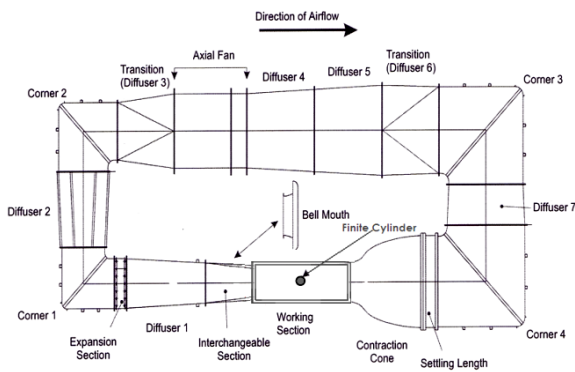


Fig. 1 Wind tunnel used fitted with the new working section

The pressure distribution measurement around the cylinder for an azimuthal angle from 0° to 180° for both the smooth cylinder and cylinder with grooves are carried out. For the later, 22 pressures tapings are installed on the cylinder circumference for a position  $Z/L = 0.833$ . The Form and dimensions of the grooves are shown in figure 2.

s indicates the width of the groove, h is the depth of the groove and L is the length of the groove.

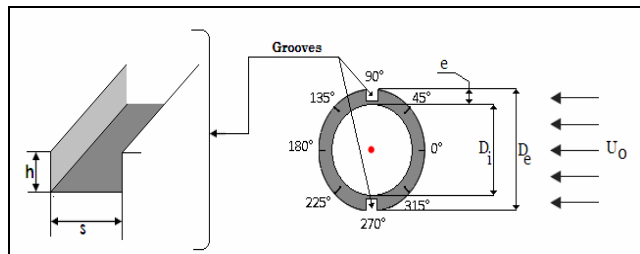


Fig. 2 Form and dimensions of the grooves

In the present work, the drag forces are measured using the TE81 balance and the pressure distributions on the cylinder

were performed using a TE44DPS differential pressure scanner.

The latter pressure scanning box allowed sequential selection of up to 20 pressure tapings.

The display unit links to a computer, loaded with DATASLIM software for data analysis and logging of results. The experiments setup is shown in figure 3. The uncertainty of the pressure measurement was 0.5 mm H2O .

All tests were carried out for a lengthening  $L/D = 10$  and  $11.5$  at various Reynolds number

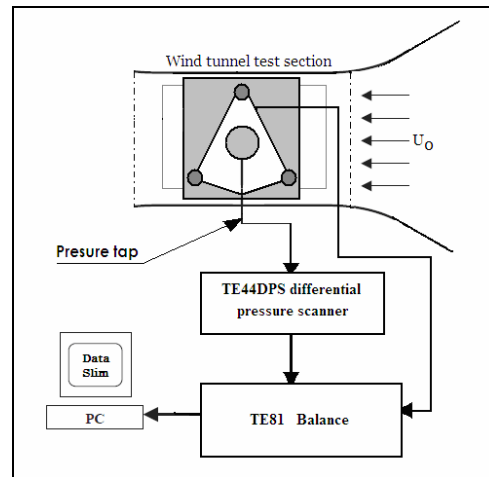


Fig. 3 Measurement hardware of drag and pressure.

III. NUMERICAL STUDY

The geometry consists of an infinite cylinder mounted horizontally on the side walls where the tow ends are fixed (the vibration effects are not considerate here). The downstream length and the upstream length are set at 11.5 of diameter; the origin of the Cartesian coordinate system is located at the centre of the base of the cylinder, the complete geometry is shown in figure 4. The geometry and the boundary conditions remain the same for all tested cylinders.

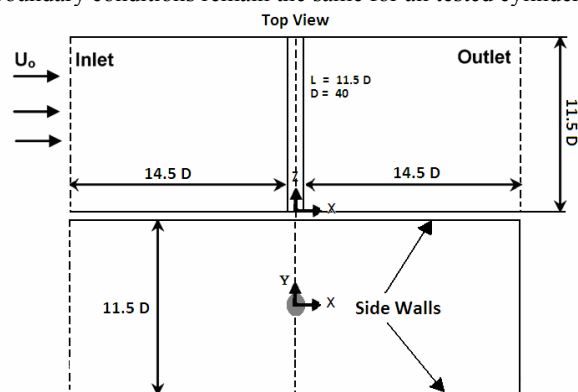


Fig. 4 Geometry under consideration of infinite cylinder

The geometry carried out numerically corresponds perfectly to the dimensions of the experimental work. In the present

study two turbulence models were tested “K- $\omega$  SST and the k- $\epsilon$ ”.

Several grids have been tested for the case of  $Re \times 10^4$  and  $AR = 11.5$  and that for the smooth cylinders.

Figure 5 shows the pressure coefficient distributions for the three grids tested;  $Re \times 10^4$  and  $AR = 11.5$  for the smooth cylinder. It is clearly seen that there is a little difference between the three grid results and the grid 2 is used in all subsequent calculations

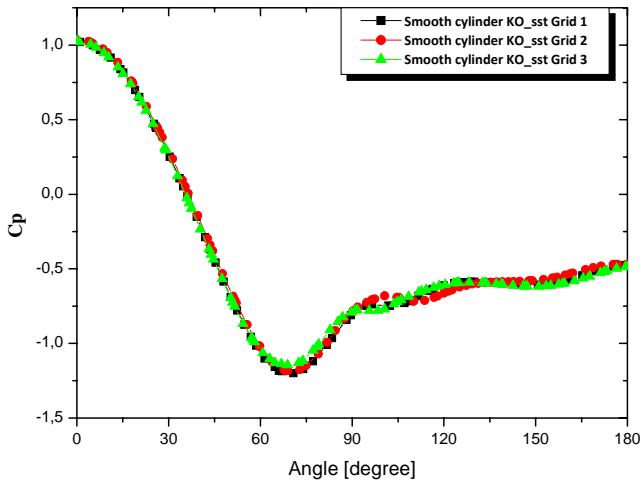


Fig. 5 Comparison of pressure coefficient around the smooth cylinder (AR 11.5) at  $Z/L = 0.883$  and  $Re = 2 \times 10^4$ , for various grids

III. RESULTS AND DISCUSSIONS

The experimental tests were performed for the following physical parameters:

- Reynolds number = 20000 (based on diameter and free stream velocity).
- Free stream velocity:  $U_0 = 7.5$  m/s.
- Two aspect ratios  $L/D = 10$  and  $L/D = 11.5$  in this study were investigated.

A. Drag distributions

The drag coefficient is calculated using the following formula:

$$C_D = \frac{2 \cdot D}{\rho \times U_0^2 \times S} \tag{1}$$

D: force of drag (-),

S: project area of the cylinder  $S = d \times L$

$P$  : Fluid density ( $Kg/m^3$ ).

L Length of the cylinder (m).

Figure 6 represents the evolution of the drag coefficient according to the Reynolds number, as well as a comparison between drag coefficients obtained for the various types of tested cylinders. Wieselsberger [16] showed that the drag force on a cylinder decreases as the aspect ratio becomes smaller and the potential gain that one can obtain on the drag reduction grows with the Reynolds number ( $C_D$  increases with

the Reynolds number). Thus, it does not appear surprising that Protas and Styczek [17] obtain a relative reduction of the drag coefficient of 15% at  $Re = 150$ , whereas Tokumaru and Dimotakis [18] obtain a reduction of 80% at  $Re = 15.000$ . Over the entire  $Re$  range ( $32 \times 10^4$  to  $2 \times 10^5$ ), the cylinders with grooves had lower  $C_D$  values than the smooth cylinder. Conversely, before their critical range, grooved cylinders had higher  $C_D$  values than the smooth cylinder. The cylinder fitted with 6 grooves shows a perfect reduction of drag when Reynolds number exceeds  $6 \times 10^4$ , but the best case it is the cylinder fitted with 2 grooves where the gain is 17.51% for  $Re = 8.6 \times 10^4$ .

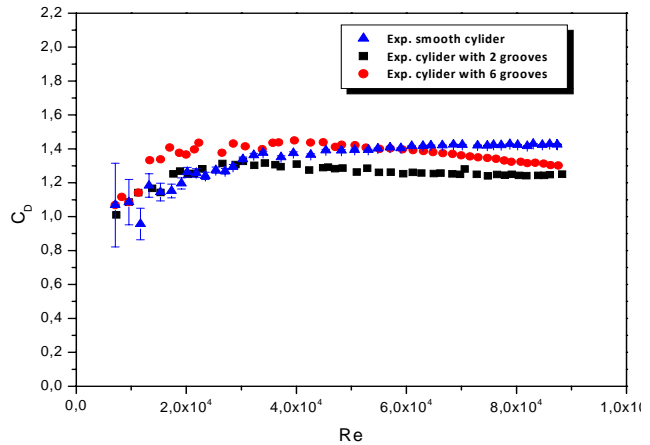
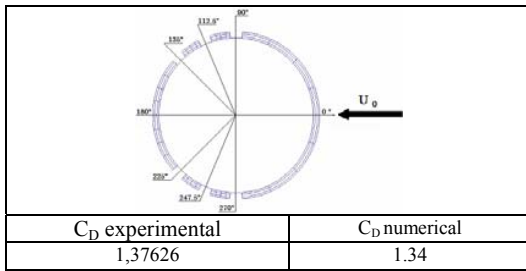


Fig. 6 Experimental drag distributions for various Reynolds numbers

Table II supplements the above comparison between the experimental and numerical results of drag coefficient for  $Re = 20000$ . It is clearly that there is a slight difference between the two results. This is related to a somewhat higher separation azimuthal angle and a lower base pressure. These observations illustrate the interaction between the upstream boundary layer and its separation with the downstream recirculation zone.

TABLE II  
EXPERIMENTAL AND NUMERICAL RESULTS OF THE DRAG FOR THE VARIOUS CYLINDERS AT  $Re = 20000$

$C_D$ experimental	$C_D$ numerical
$1,26227 \pm 0,02913$	1.4
$C_D$ experimental	$C_D$ numerical
1,24986	1.27



### B. Pressure coefficient distribution

The difference in pressure between the pressure,  $P$ , and the static pressure,  $P_{ref}$ , is divided by the dynamic pressure to obtain the pressure coefficient, for correlations and the discussion to follow; the coefficient of pressure is defined as:

$$C_p = \frac{p - p_{ref}}{0.5(\rho \cdot U_0^2)} \quad (2)$$

Figure 7 shows pressure coefficient comparison around the surface of the smooth cylinder for an aspect ratio  $AR = 10$  obtained in the present study and the experimental of Park and Lee [19] for plan  $Z/L = 0.833$  and Reynolds number  $Re = 20.000$ . There is a satisfactory agreement between the present results and those of reference [19]. It is clearly seen that the numerical results is located between two experimental curves.

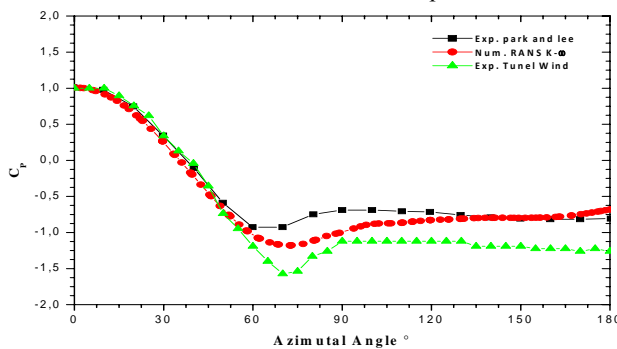


Fig. 7 comparison of pressure coefficient for a smooth cylinder ( $AR = 10$  and  $Z/L = 0.833$ )

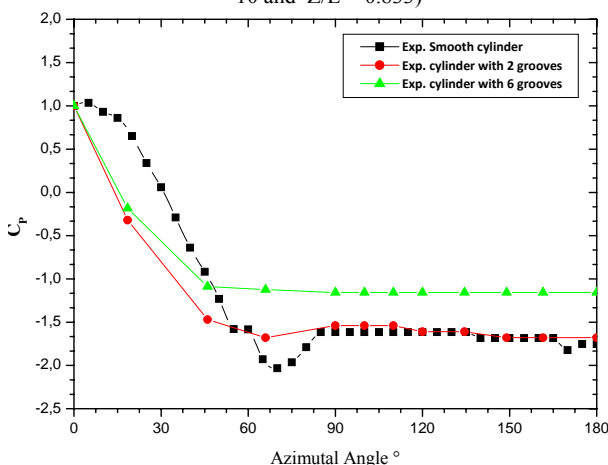


Fig. 8 Pressure coefficient distributions for  $Z/L = 0.883$  experimental investigation

The distribution of pressure coefficient at  $Re = 20.000$  and  $AR = 11.5$  for the smooth cylinder and the cylinders with grooves are shown in figure 8. There is greater pressure recovery for cylinders with grooves than for the smooth cylinder. The cylinders with grooves have greater negative pressures on the sides of the cylinder. The pressure drag is reduced due to this large reduction in the pressure on the front surface of the cylinders with grooves. As the number of grooves increases, the pressure coefficient decreases on the front face of the cylinder ( $\theta \geq 45^\circ$ ), therefore, in comparison with the system without grooves (smooth cylinders), the flow separation point, at which the fluid experiences an adverse pressure is delayed. The pressure coefficient distribution depends somewhat on the orientation and the number of grooves to the flow. The profiles of the pressure coefficient display a  $C_p = c^{te}$  on the portion  $90^\circ < \theta < 180^\circ$  what is explained by the existence of an alley of Von Kàrmàn, what indicates that the 2D flow is reached. It is seen that  $C_p$  grows in algebraic value as it approaches the downstream stagnation point what is coherent with the experimental results of Park & Lee [19].

### IV. CONCLUSION

The flow around a circular cylinder was controlled by using grooves; the results obtained seem to agree rather well with the experimental and theoretical data already gathered, in particular on the distribution of pressure around the examined cylinders. Following this investigation; it was possible to put the light on the following points:

- The importance of the experimental investigation in order to clear up the physical phenomena described by the theory.
- the evaluation and analysis of the distribution of the pressure on the surface of the cylinder,
- The pressure drag reduction is due to the decreasing pressure in the front face of the circular cylinder and the moving aft of the separation point on the circular cylinder.
- The drag form is reduced by using grooves.

### REFERENCES

- [1] Sakamoto et al., 1991 H. Sakamoto, K. Tan and H. Haniu, An optimum suppression of fluid forces by controlling a shear layer separated from a square prism, *Journal of Fluids Engineering* 113 (1991), pp. 183–189
- [2] N. Fujisawa, G. Takeda. 2003. Flow control around a circular cylinder by internal acoustic excitation Original Research Article. *Journal of Fluids and Structures*, Volume 17, Issue 7, June 2003, Pages 903-913.
- [3] Igarashi, T., Tsutsui, T., 1989. Flow control around a circular cylinder by a new method (2nd report, Fluids forces acting on the cylinder). *Trans. JSME* 55 (511), 708–714 (in Japanese).
- [4] Igarashi, T., Tsutsui, T., 1991. Flow control around a circular cylinder by a new method (3rd report, properties of the reattachment jet). *Trans. JSME* 57 (533), 8–13 (in Japanese).
- [5] Lee, S.J., Lee, S.I., Park, C.W. 2004 Reducing the drag on a circular cylinder by upstream installation of a small control rod. *Fluid Dynamics Research*, 34, p.233-250.
- [6] Lee, H.B., Lee, S.J., 1995. Flow structure of modified cylinder wake by a small control cylinder. *Proceedings of the Sixth Asian Congress of Fluid Mechanics* 2, 1608–1611.

- [7] Tsutsui, T., Igarashi, T., 1995. Drag reduction of a circular cylinder (2nd report, effect of Reynolds number). Trans. JSME 61 (586), 2069–2075 (in Japanese).
- [8] Tsutsui, T., Igarashi, T., 1996. Enhancement of heat transfer and reduction of drag of a circular cylinder (flow control using a small rod). Trans. JSME 62 (597), 1802–1809 (in Japanese).
- [9] Mahir, N., Rockwell, D., 1996. Vortex formation from a forced system of two cylinders. Part II: side-by-side arrangement. *J. Fluids Struct.* 10, 491–500.
- [10] Zdravkovich, M.M., 1977. Review of flow interference between two circular cylinders in various arrangements. Trans. ASME J. Fluids Eng. 99, 618–633.
- [11] Igarashi, T., 1997. Drag reduction of a square prism by flow control using a small rod. *J. Wind Eng. Ind. Aerodyn.* 69–71, 141–153.
- [12] Mittal, S., Kumar, V., Raghuvanshi, A., 1997. Unsteady incompressible flows past two cylinders in tandem and staggered arrangements. *Int. J. Numer. Methods Fluids* 25 (11), 1315–1344.
- [13] Sakamoto, H., Haniu, H., 1994. Optimum suppression of fluid forces acting on a circular cylinder. *J. Fluids Eng.* 116, 221–227.
- [14] E. Coustols. 2001 effect of grooved surfaces on the structure of a turbulent boundary layer. *Mec. Ind.* 2.421-234. Edition scientifique et médicale Elsevier SAS. S1296-2139(01)01125-3/FLA.
- [15] S. Talley and G. Mungal. 2002 Flow around cactus-shaped cylinders. Center for Turbulence Research Annual Research Briefs.
- [16] Wieselsberger, C. 1922 New data on the laws of fluid resistance. NACA Tech. Rep. TN-84.
- [17] B. Protas and A. Styczek, 2002 "Optimal Rotary Control of the Cylinder Wake in the Laminar Regime", *Physics of Fluids* 14(7), 2073-2087, 2002.
- [18] Tokumaru, P.T., and Dimotakis, P.E. 1991. Rotary oscillation control of cylinder wake. *Journal of Fluid Mechanics*, Vol. 224, pp. 77-90.
- [19] Park, C. W., Lee, S. J. 2000. Free end effect on the wake flow structure behind a finite circular cylinder. *J. Wind Eng. Ind. Aero.* 88. 231-246.